Gas Permeation Properties of Ion-Exchanged Faujasite-Type Zeolite Membranes

K. Kusakabe, T. Kuroda, K. Uchino, Y. Hasegawa, and S. Morooka
Dept. of Materials Physics and Chemistry, Kyushu University, Fukuoka 812-8581, Japan

NaY-type zeolite membranes were synthesized on a porous support tube by a hydrothermal process. The membranes were ion-exchanged with Li^+ and K^+ ions, and permeances through the membranes were determined for an equimolar mixture of CO_2 and N_2, as well as for single-components thereof, at a temperature range of 0−400°C. The permeance to CO_2 showed a maximum at 100°C, but CO_2/N_2 selectivity decreased with increasing temperature. The zeolite membranes that were exchanged with K^+ and Li^+ ions gave higher and lower CO_2/N_2 selectivities, respectively, than were found for the NaY-type membrane. The permeation properties of the ion-exchanged zeolite membranes were analyzed using a sorption−diffusion model. The high CO_2/N_2 selectivity of the K-exchanged membranes can be explained by the decrease in N_2 sorptivity for the mixed feed.

Introduction

Zeolite membranes have recently been applied to the separation of constitutional isomers (Vroon et al., 1996; Funke et al., 1997a; Kusakabe et al., 1997a; Nomura et al., 1997; Coronas et al., 1998), the recovery of carbon dioxide from combustion gas (Kusakabe et al., 1997b, 1998a; Poshusta et al., 1998), and the pervaporation of alcohol−water mixtures (Kondo et al., 1997; Sano et al., 1997; Kita, 1998; Nomura et al., 1998). These separation processes are based on the affinity between pore walls and molecules, as well as the size of molecules permeating through the membrane (Bakker et al., 1996, 1997; Funke et al., 1997b; Burggraaf et al., 1998). Most of the zeolitic membranes that have been studied to date are composed of MFI-type zeolites, such as silicalite and ZSM-5. Defect-free MFI-type zeolite membranes show CO_2/N_2 selectivities of the order of 10 (Kusakabe et al., 1997a), which are insufficient for practical uses. Kusakabe et al. (1997b) prepared NaY-type zeolite membranes and determined the permeation rates for CO_2/N_2 systems. When an equimolar mixture of CO_2 and N_2 was fed onto the feed side, the CO_2 permeance was nearly equal to that found for single-component systems. However, the N_2 permeance was greatly decreased when this mixture was fed in, especially at lower permeation temperatures. The permeance of CO_2 at 30°C was $(0.5–6)\times10^{-6}$ $mol\cdot m^{-2}\cdot s^{-1}\cdot Pa^{-1}$, and the CO_2/N_2 selectivity was 20−100. NaY-type zeolite membranes, which were ion-exchanged with various alkali and alkali-earth cations, showed permeation properties that depended on the exchanged ions (Kusakabe et al., 1998a).

Gas permeation through porous inorganic membranes is often explained by Knudsen diffusion, surface diffusion, and molecular sieving. However, differences in permeances for single-component and mixed systems cannot be fully explained by these three mechanisms (Kusakabe et al., 1997b, 1998b; Sea et al., 1997). As shown in Figures 1 and 2, the behavior of molecules on the surface of the membrane and in the pores must be considered separately (Barrer, 1990; Bakker et al., 1996; Kusakabe and Morooka, 1998). The majority of the molecules incident from the gas phase rebound and do not enter the pores, as shown in Figure 1a. The probability of small molecules entering the pore is higher than that of larger molecules. However, molecules that are adsorbed to the surface migrate by surface diffusion and preferentially enter the pore, as shown in Figure 1b. When the size of the pore is roughly the same as the size of the molecules to be separated, the membrane is capable of distinguishing molecules based on their sizes, as shown in Figure 1c, but the permeation rate via a molecular-sieving mechanism is very low (Morooka et al., 1995).

Correspondence concerning this article should be addressed to S. Morooka.

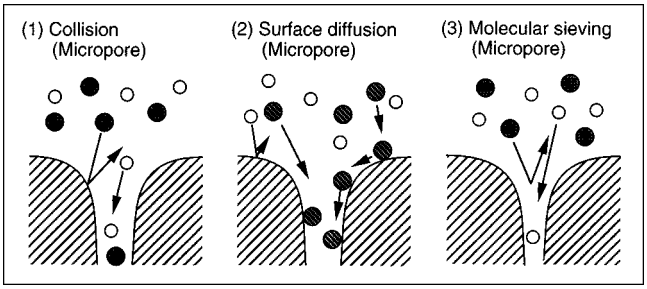

Figure 1. Molecular flow at the entrance to a micropore.

The permeation mechanism through an inorganic membrane can be estimated from an Arrhenius plot of permeation rates. When Henry's law is applied to the adsorption of permeating molecules, the flux through the micropores, J, can be described as follows (Burggraaf et al., 1996):

$$J \propto D_0 \exp\left[-(E_D - Q_{ad})\right], \tag{1}$$

where D_0 is the diffusivity at infinite temperature, E_D is the diffusional activation energy, and Q_{ad} is the heat of adsorption. The permeation of less adsorptive molecules in the micropores is controlled by activated diffusion, and the apparent activation energy for the permeation is positive. For adsorptive molecules, the permeation is controlled by the surface-diffusion mechanism, and the apparent activation energy is negative. Furukawa and Nitta (1997) simulated gas permeation through nanoporous carbon membranes by nonequilibrium molecular dynamics, and showed that molecules were transported by the surface flow near the pore wall. The transient permeabilities of light hydrocarbon through a silicalite membrane were investigated and modeled by the Maxwell–Stefan equation (Bakker et al., 1996; Krishna and van den Broeke, 1995), which was applied to the surface diffusion in a micropore by Krishna and Wesselingh (1997). Bakker et al. (1997) and Nishiyama et al. (1997) proposed a parallel diffusion model, assuming that molecules diffused through a micropore in the center region by activated gas diffusion and along the peripheral region of the pore by surface diffusion. Bakker et al. (1997) also analyzed the permeation of light hydrocarbons through a silicalite membrane and found that activation energies were comparable for the activated gas- and surface-diffusion mechanisms. However, NaY-type zeolite membranes have larger pores than silicalite membranes. Thus the contribution of activated diffusion may be significant even for adsorptive molecules.

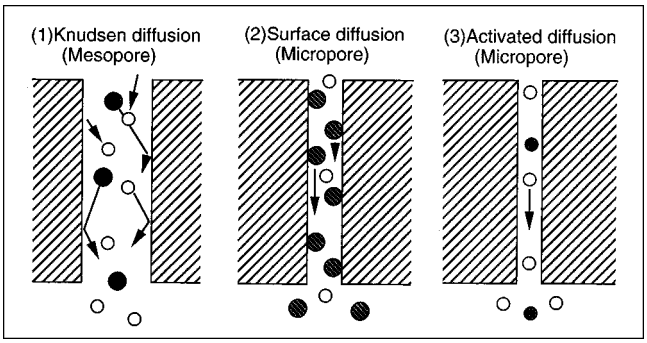

Figure 2. Effect of pore size on permeation through a microporous membrane.

In this article, ion-exchanged Y-type zeolite membranes (Kusakabe et al., 1998a) were synthesized, and permeation rates for CO_2/N_2 systems were determined over a wide range of permeation temperatures. Permeation properties for mixtures of CO_2/H_2, CH_4/H_2, C_2H_6/H_2 and C_3H_8/H_2 were also determined, and these data were compared with the CO_2/N_2 systems. Adsorbed amounts of CO_2 and N_2 on the ion-exchanged Y-type zeolite membranes were measured, and the relationship between permeation and adsorption was discussed based on a sorption–diffusion model.

Experimental Methods

Synthesis of membranes

A continuous Y-type zeolite membrane was hydrothermally formed on a porous α-alumina support tube (NOK Corp., Japan). The dimensions of the support tube were length, 200 mm; outside diameter, 2.8 mm; inside diameter, 1.9 mm; void fraction, 0.40; and pore size, 120–150 nm. The outer surface of the support tube other than the permeation central portion, which was 10–15 mm in length, was glazed with a $SiO_2/Na_2O/B_2O_3$ sealant (Nippon Electric Glass, #GA-4), and calcined at 750°C for 60 min. In order to avoid dissolution of the glass sealant in the alkaline solution during the hydrothermal reaction described below, the sealed parts were wrapped with a polytetrafluorocarbon tape and further coated with a hydrofluorocarbon polymer. The zeolite membranes thus formed on the glass-sealed support tube were used for permeation tests at 200–400°C. For permeation tests at 0–130°C, zeolite membranes were synthesized over the entire 200-mm length of the support tube without glass sealing. Each tube was then cut into six 30-mm-long membranes. The end of each membrane was connected with epoxy resin to a stainless-steel holder 10 cm in length, and the membrane was then subjected to permeation tests.

An aqueous solution of water glass, sodium aluminate, and NaOH was homogenized by stirring for 4 h at room temperature. The initial composition of the solution was Al_2O_3:SiO_2:Na_2O:H_2O = 1:12.8:17:975 on a molar basis. This solution resulted in the formation of a Y-type zeolite that had a Si/Al composition of 1.5. The outer surface of the support tube was rubbed with NaX (Tosoh Corp., #F-9; Si/Al = 1.25, crystal size = 3–5 μm) or NaY (Tosoh Corp., #HSZ-320NAA; Si/Al = 2.8, crystal size = 0.5 μm) zeolite particles to implant seeds for nucleation. After the porous support tube was rubbed with the zeolite particles, it was positioned horizontally in a tubular autoclave (10 mm ID and 300 mm in length). The reaction was carried out at 90°C for 24 h. After the synthesis, the tube was thoroughly washed with distilled water and dried in air at ambient temperature. Details of the preparation procedures have been described elsewhere (Kusakabe et al., 1998a).

The 200-mm-long NaY-type zeolite membrane was cut into six 30-mm-long pieces, which were then subjected to ion-exchange treatment and permeation tests. Cation exchange of the NaY-type zeolite membranes was carried out in a 0.1-mol·L^{-1} solution of LiCl or KCl at 80°C for 4 h. After the

ion-exchange treatment, the membranes were thoroughly washed with distilled water and then air dried at ambient temperature. The morphology of the membranes was observed by scanning electron microscopy (FESEM, Hitachi S-900). The crystal structure was determined by X-ray diffraction (XRD, Rigaku RINT-2500 KS), using the NaY-type zeolite particles (Tosoh Corp., #HSZ-320NAA) as the reference. The Si/Al ratio and the extent of ion exchange in the membranes was determined using an energy-dispersive X-ray analyzer (EDXA, Kevex Delta Class).

Permeation and adsorption experiments

Permeation tests were performed at 0–400°C. The permeation cell, in which a zeolite membrane was fixed, was placed in an electric furnace. The heating and cooling rates of the cell were maintained at 1°C/min to prevent thermal collapse of the zeolite membrane. For the case of the permeation test at 0°C, the permeation cell was placed into an ice-cold water bath. Single-component CO_2 and N_2 and an equimolar mixture of the two were fed on the feed side (outside) of the membrane. Permeated gases on the permeated side (inside) were swept out using a stream of helium, and the concentrations of permeants were determined using a TCD-GC. All of the flow rates on the feed and permeate sides were determined with soap film flowmeters. The partial pressure of the permeants on the permeate side was maintained below 1 kPa by varying the sweep flow rate. Total pressure on both sides of the membrane was maintained at 101.3 kPa throughout the experiment. Permeance was calculated from the following equation:

$$\text{Permeance} = \frac{(\text{mole of gas transferred per unit time})}{(\text{membrane area})(\text{partial pressure difference})}. \quad (2)$$

Permeance was also determined using an equimolar mixture of CO_2/H_2, CH_4/H_2, C_2H_6/H_2, or C_3H_8/H_2. Selectivity was defined by the ratio of permeances. The partial pressure difference of the permeants between the feed and permeate sides was calculated by logarithmically averaging the differences at the inlet and outlet on the permeates side.

NaY-type crystals were prepared under the same conditions as were used for the synthesis of zeolite membranes. Each sample was outgassed *in vacuo* at 200°C for 8 h, and adsorption isotherms for CO_2 and N_2 were determined at 35°C and 0–101.3 kPa using a constant-volume adsorption unit. Micropore volumes of zeolites were calculated from desorption isotherms of argon using an adsorption unit (Micromeritics, ASAP 2010).

Results and Discussion

Figure 3 shows the relationship between permeances and selectivity for the CO_2/N_2 systems, for the Y-type zeolite membranes synthesized after seeding with the NaX or NaY zeolite particles. Selectivities of the membranes synthesized with seeding with the NaY zeolite particles were higher than those seeded using the NaX particles. The mesopores in the support were plugged by finer NaY particles and, as a result, zeolite membranes with fewer defects were obtained.

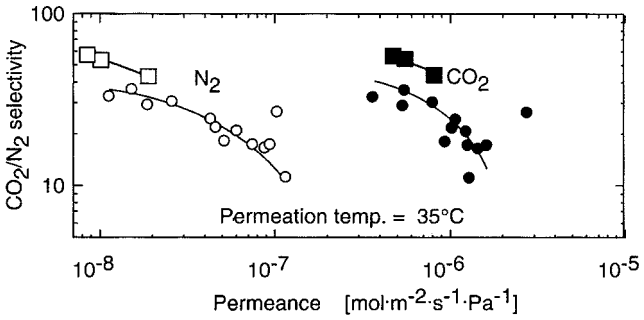

Figure 3. Relationship between CO_2/N_2 selectivity and permeance to N_2 and CO_2 at 35°C.

Seeds: □ and ■ NaY zeolite; ○ and ● NaX zeolite.

Figure 4 shows the effect of permeation temperature on the permeance and selectivity of the NaY-type zeolite membranes for an equimolar mixture of CO_2 and N_2. The gaps observed in the data collected at 40°C were due to the fact that different membranes synthesized under the identical conditions were used for permeation tests in the temperature ranges lower and higher than 40°C. Permeances to CO_2 and N_2 greatly increased with increasing permeation temperature over the range of 0–40°C. In the 40–400°C temperature range, however, the permeances to CO_2 and N_2 initially increased and then decreased. The maximum permeances to CO_2 and N_2 appeared at 100 and 200°C, respectively. The CO_2/N_2 selectivity decreased with increasing permeation temperature from a value of 100 at 0°C to 1.7 at 400°C.

The amount of gas adsorbed on the zeolite decreases, while the diffusivity of the gas increases with increasing permeation temperature. The maxima in permeances can be rationalized based on a combination of adsorption and diffusion (Bakker

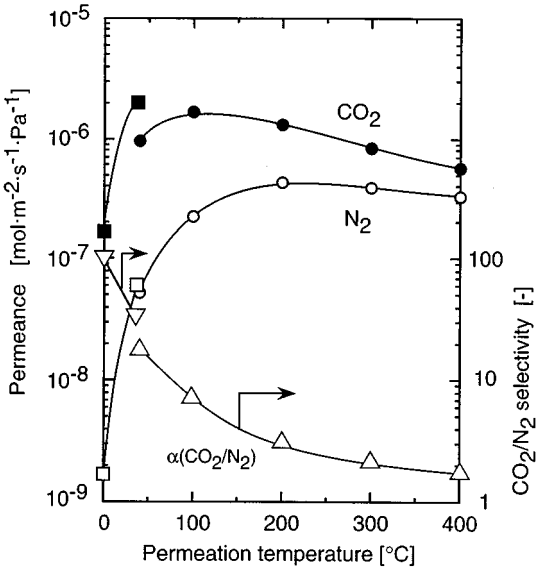

Figure 4. Effect of permeation temperature on permeance and CO_2/N_2 selectivity for NaY-type zeolite membranes.

□ ■ ▽ membrane A; ○ ● △, membrane B.

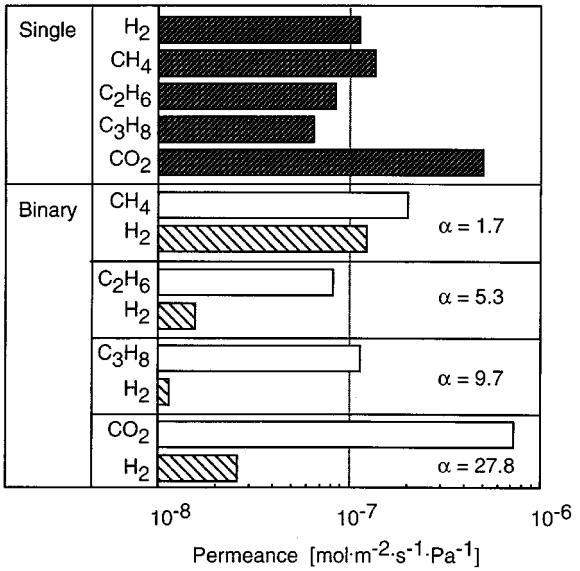

Figure 5. Permeances and selectivities at 35°C for NaY-type zeolite membranes.

et al., 1996, 1997; Vroon et al., 1998; Coronas et al., 1997). The molecular transport of the Y-type zeolite in a micropore can be described by both the activated diffusion in the confined space and the surface transport due to the hopping movement of molecules between adsorption sites (Okazaki et al., 1981), as a result of the relatively wide pore space.

Figure 5 shows the permeances of the NaY-type zeolite membrane for equimolar mixtures of CO_2/H_2, CH_4/H_2, C_2H_6/H_2, and C_3H_8/H_2, as well as pure samples of these individual gases, at a permeation temperature of 35°C. The kinetic diameters of the permeances are on the order of C_3H_8 (0.43 nm) > C_2H_6 (0.39 nm) > CH_4 (0.38 nm) > CO_2 (0.33 nm) > H_2 (0.29 nm) (Breck, 1974). This order is not directly related to that of the permeances to single-component gases. The permeance to CO_2 is much higher than that to H_2. These results are consistent with the findings reported for an MFI-type zeolite membrane (Bakker et al., 1997). Permeance to H_2, which was only weakly adsorbed on the pore wall, greatly decreased when accompanied by an adsorbing gas such as CO_2, C_2H_6, and C_3H_8.

Adsorption isotherms of single-component CO_2 and N_2 were determined for the ion-exchanged Y-type zeolites at 35°C. Approximately 20 and 30% of the initial Na ions in the zeolite were exchanged for Li^+ and K^+ ions, respectively. As shown in Figure 6, the amount of CO_2 adsorbed was higher than that of N_2. The exchange of Na^+ ions for Li^+ ions increased the adsorbed amounts of both CO_2 and N_2, and the exchange with K^+ ions increased that of CO_2, but decreased that of N_2. Equilibrium data of pure CO_2 and N_2 were correlated using the Langmuir equation:

$$q_i = q_{is} K_i P_i / (1 + K_i P_i). \quad (3)$$

The adsorbed amount of component i at saturation, q_{is}, and the Langmuir coefficient of component i, K_i, are summarized in Table 1.

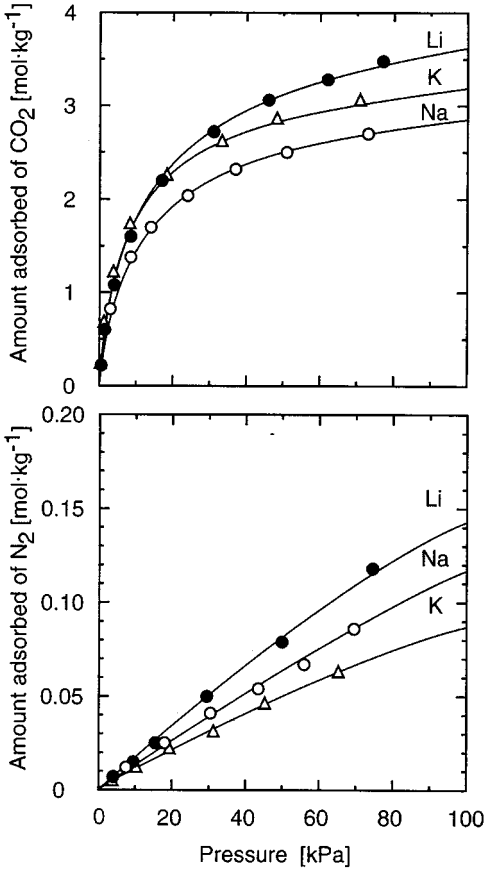

Figure 6. Adsorption isotherms of CO_2 and N_2 at 35°C for ion exchanged Y-type zeolites.

The solid lines are calculated from the Langmuir isotherm equation using parameters indicated in Table 1.

Figure 7 shows the permeances of the ion-exchanged Y-type zeolite membranes for the single and binary CO_2/N_2 systems. Compared to the permeances for the single-component systems, the CO_2 permeance for the binary mixture was high, but that for N_2 was low. Consequently, the selectivity of CO_2 to N_2 increased when the mixture was fed in. The N_2 permeances of the ion-exchanged membranes were on the order of $Li^+ > Na^+ > K^+$. Table 2 shows the permeation properties of the zeolite membranes synthesized independently: F1, F2, and F3. Although the permeances were dependent on the samples, the selectivity of CO_2/N_2 was

Table 1. Adsorbed Amounts at Saturation and Langmuir Coefficients of the Ion-Exchanged Y-Type Zeolites

Zeolite Ion	Gas	q_{is} (mol·kg^{-1})	K_i (Pa^{-1})
Li	CO_2	4.1	6.7×10^{-5}
	N_2	0.5	0.4×10^{-5}
Na	CO_2	3.1	8.6×10^{-5}
	N_2	0.4	0.4×10^{-5}
K	CO_2	3.4	10.1×10^{-5}
	N_2	0.3	0.4×10^{-5}

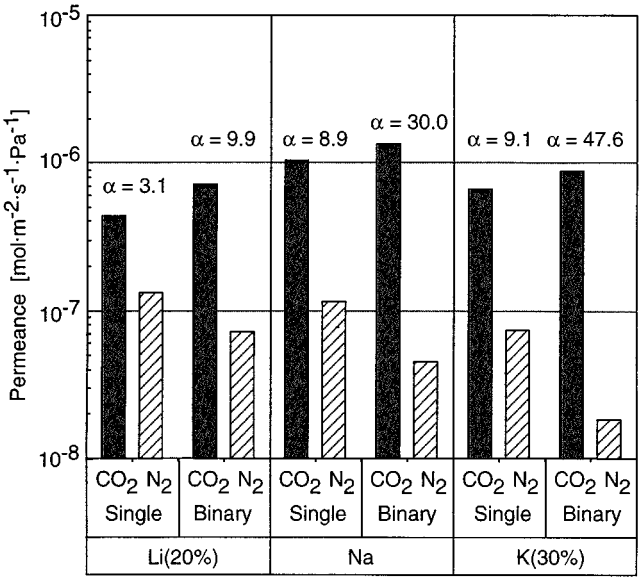

Figure 7. Effect of ion-exchange on permeances and selectivities at 35°C for Y-type zeolite membranes.

consistently on the order of $K^+ > Na^+ > Li^+$ for the single-component systems as well as for the mixed feeds.

Permeances are defined based on the partial-pressure difference between the feed and permeate sides. Since the concentration in the membrane is not proportional to the partial pressure in the gas phase, permeances for mixed-component systems are not equal to those for single-component systems, as indicated in Figure 7. To estimate the permeation rates quantitatively, permeances to CO_2 and N_2 through the zeolite membranes are analyzed based on a modified sorption–diffusion model. The amount of component i adsorbed, q_i, indicated in Figure 6, is modified to the adsorbed mass per zeolite volume by multiplying the density of the zeolite layer, ρ. The adsorbed amount of component i in a mixture of i and j can be calculated from the Langmuir adsorption model (Ruthven, 1984).

$$q_i = q_{is} K_i P_i / (1 + K_i P_i + K_j P_j). \tag{4}$$

For a porous inorganic membrane, gas molecules are located not only on the pore wall by adsorption but also in the pore space, as shown in Figure 1. The gas concentration in the pore space is described by the ideal gas law. Thus, the overall concentration of a permeant i in the membrane pores can be described as

$$C_i = q_i \rho + \epsilon f P_i / (RT), \tag{5}$$

where ϵ is the voidage of the zeolite layer, and P_i is the partial pressure of component i. The correction factor f, which is due to the attractive force in the pore, can be larger than unity. For simplicity, however, the f is assumed to be unity in the present study. The density of the NaY-type zeolite is estimated to be 1.5×10^3 kg·m^{-3} from the frame density (Breck, 1974) and the Si/Al ratio. The voidage is estimated from the measured micropore volume and is 0.16 for the NaY-type zeolite. The sorptivity of the membrane can be defined as

$$S = (C_{\text{feed}} - C_{\text{permeate}}) / (P_{\text{feed}} - P_{\text{permeate}}). \tag{6}$$

The subscripts, feed and permeate, refer to the feed and permeate sides of the membrane, respectively. The adsorbed amount of N_2 at a given partial pressure on the feed and permeate sides (for instance, 101 kPa and 0.9 kPa) is calculated from the adsorption isotherm shown in Figure 6. Substituting q_i in Eq. 5 with the value calculated from Eq. 3 or Eq. 4, and using a zeolite density $\rho = 1{,}510$ kg·m^{-3} and the voidage $\epsilon = 0.16$, the surface concentrations of the N_2 on the feed and permeate sides are estimated to be 190 and 0.06 mol·m^{-3}, respectively. The sorptivity is then calculated from Eq. 6 (in this case, 1.9×10^{-3} mol·m^{-3}·Pa^{-1}).

The zeolite layer, which is effective for separation, is formed in the macropore of the support. The thickness of the zeolite layer used in this study, as estimated from SEM observations, is approximately 3 μm. The permeability coefficient can then be calculated by multiplying the permeance by the thickness. The diffusion coefficient is calculated from

Table 2. Permeances of the Ion-Exchanged Y-Type Membranes for an Equimolar Mixture of CO_2 and N_2 at 35°C

Memb. Ion	CO_2 Permeance (mol·m^{-2}·s^{-1}·Pa^{-1})	N_2 Permeance (mol·m^{-2}·s^{-1}·Pa^{-1})	Selectivity
F1(Li)	16×10^{-7}	27×10^{-8}	5.8
F3(Li)	7.1×10^{-7}	7.8×10^{-8}	9.0
F1(Na)	9.1×10^{-7}	2.4×10^{-8}	39
F2(Na)	3.3×10^{-7}	1.4×10^{-8}	24
F3(Na)	13×10^{-7}	4.4×10^{-8}	30
F1(K)	13×10^{-7}	1.9×10^{-8}	67
F2(K)	4.2×10^{-7}	1.2×10^{-8}	35
F3(K)	8.8×10^{-7}	1.8×10^{-8}	48

Table 3. Permeabilities, Sorptivities, and Diffusivities of the Ion-Exchanged Y-Type Zeolite Membranes for Single-Component Systems at 35°C

Zeolite Ion	Gas	S (mol·m^{-3}·Pa^{-1})	D (m^2·s^{-1})	Q_p (mol·m·m^{-2}·s^{-1}·Pa^{-1})
Li	CO_2	3.7×10^{-2}	3.6×10^{-11}	1.3×10^{-12}
	N_2	2.4×10^{-3}	1.7×10^{-10}	4.0×10^{-13}
Na	CO_2	2.7×10^{-2}	1.1×10^{-10}	3.1×10^{-12}
	N_2	1.9×10^{-3}	1.8×10^{-10}	3.5×10^{-13}
K	CO_2	2.5×10^{-2}	8.1×10^{-11}	2.0×10^{-12}
	N_2	1.6×10^{-3}	1.4×10^{-10}	2.2×10^{-13}

Table 4. Sorptivities, Diffusivities, and Permeabilities of the Ion-Exchanged Y-Type Zeolite Membranes for an Equimolar Mixture of CO_2 and N_2 at 35°C

Zeolite Ion	Gas	S (mol·m^{-3}·Pa^{-1})	D (m^2·s^{-1})	Q_p (mol·m·m^{-2}·s^{-1}·Pa^{-1})
Li	CO_2	8.4×10^{-2}	2.5×10^{-11}	2.1×10^{-12}
	N_2	7.1×10^{-4}	3.3×10^{-10}	2.4×10^{-13}
Na	CO_2	5.5×10^{-2}	7.3×10^{-11}	4.0×10^{-12}
	N_2	5.5×10^{-4}	2.4×10^{-10}	1.3×10^{-13}
K	CO_2	6.4×10^{-2}	4.1×10^{-11}	2.6×10^{-12}
	N_2	4.0×10^{-4}	1.4×10^{-10}	5.5×10^{-14}

sorptivity and the permeability coefficient.

$$D = Q_p/S. \tag{7}$$

Tables 3 and 4 summarize sorptivities, diffusivities, and permeabilities for CO_2 and N_2 at 35°C in the ion-exchanged Y-type zeolite membranes for the single-component and binary-mixture systems, respectively. The diffusivities for N_2 are higher than those for CO_2 for both systems. The same tendency was reported for single-component permeation through silicalite membranes (Bakker et al., 1997). The values of N_2 diffusivities are not greatly dependent on exchanged cation species and are $(1.4-1.8)\times10^{-10}$ m^2·s^{-1} for the single-component systems and $(1.4-3.3)\times10^{-10}$ m^2·s^{-1} for the binary system. However, the CO_2 diffusivities are dependent on adsorption properties, which vary with the cation species. Kapteijn et al. (1995) determined Maxwell–Stefan diffusivities for hydrocarbons in silicalite. The values of CH_4, C_2H_6, and C_3H_8 at 27°C were of the order of 10^{-9}, 10^{-10} and 10^{-11} m^2·s^{-1}, respectively. Talu et al. (1998) evaluated directional diffusivities for a series of *n*-alkanes in a silicalite single crystal. The diffusivities of CH_4 were close to the value reported by Kapteijn et al. (1995). Bakker et al. (1997) described single-component permeation rates through a silicalite membrane based on activated diffusion and surface diffusion. The diffusivities for N_2 and CO_2 at 30°C coincided approximately with the values listed in Table 3. Masuda et al. (1996) determined the diffusivities of hydrocarbons of NaY-type zeolite crystals as $10^{-14}-10^{-15}$ m^2·s^{-1}. Their values are very much smaller than those obtained in the present study.

The selectivity of CO_2 to N_2 may be expressed by the following equation, provided sorptivity and diffusivity function independently:

$$\alpha = Q_{p,CO_2}/Q_{p,N_2} = \left(D_{CO_2}/D_{N_2}\right)\left(S_{CO_2}/S_{N_2}\right) = \alpha_D\,\alpha_S. \tag{8}$$

Table 5. Ratios of Sorptivities and Diffusivities of the Ion-Exchanged Y-Type Zeolite Membranes for Single-Components and an Equimolar Mixture of CO_2 and N_2 at 35°C

Zeolite Ion	System	α_S	α_D	$Q_{p,CO_2}/Q_{p,N_2}$
Li	Single	15	0.21	3.1
	Binary	119	0.076	9.0
Na	Single	14	0.62	8.9
	Binary	100	0.30	30
K	Single	15	0.59	9.1
	Binary	160	0.30	48

Table 5 shows the values of α_S and α_D for the ion-exchanged membranes, which suggest that the CO_2/N_2 selectivities were largely controlled by the ratio of sorptivities. However, the small CO_2/N_2 selectivity of the membrane exchanged with Li^+ ions (Li exchange yield = 20%) was dominated by the ratio of diffusivities.

Conclusions

The CO_2/N_2 selectivity of the NaY-type zeolite membrane for binary systems was in the 20–50 range at room temperature and decreased with increasing permeation temperature. Preferential transport of adsorptive molecules through the membranes was also confirmed for the CO_2/H_2, C_2H_6/H_2, and C_3H_8/H_2 systems. The permeation properties of the ion-exchanged zeolite membranes were then analyzed using a modified sorption–diffusion model. The high CO_2/N_2 selectivities for the binary mixed feed were caused by an increase in the selective sorption of CO_2.

Acknowledgments

This work was supported by the Ministry of Education, Science, Sports and Culture of Japan and the New Energy and Industrial Technology Development Organization (NEDO) of Japan. We also acknowledge the support of NOK Corporation, Kyocera Corporation, Tosoh Corporation, and Nippon Electric Glass Corporation.

Notation

P_i = partial pressure of gas, Pa
R = gas constant, J·mol^{-1}·K^{-1}
T = temperature, K

Literature Cited

Bakker, W. J. W., F. Kapteijn, J. Poppe, and J. A. Moulijn, "Permeation Characteristics of a Metal-Supported Silicalite-1 Zeolite Membrane," *J. Memb. Sci.*, **117**, 57 (1996).

Bakker, W. J. W., L. J. P. van den Broeke, F. Kapteijn, and J. A. Moulijn, "Temperature Dependence of One-Component Permeation Through a Silicalite-1 Membrane," *AIChE J.*, **43**, 2203 (1997).

Barrer, R. M., "Porous Crystal Membranes," *J. Chem. Soc. Faraday Trans.*, **86**, 1123 (1990).

Breck, D. W., *Zeolite Molecular Sieves*, Wiley, New York (1974).

Burggraaf, A. J., and L. Cot, *Fundamentals of Inorganic Membrane Science and Technology*, Elsevier, Amsterdam (1996).

Burggraaf, A. J., Z. A. E. P. Vroon, K. Keizer, and H. Verweij, "Permeation of Single Gases in Thin Zeolite MFI Membranes," *J. Memb. Sci.*, **144**, 77 (1998).

Coronas, J., J. L. Falconer, and R. D. Noble, "Characterization and Permeation Properties of ZSM-5 Tubular Membranes," *AIChE J.*, **43**, 1797 (1997).

Coronas, J., R. D. Noble, and J. L. Falconer, "Separations of C_4 and C_6 Isomers in ZSM-5 Tubular Membranes," *Ind. Eng. Chem. Res.*, **37**, 166 (1998).

Funke, H. H., A. M. Argo, J. L. Falconer, and R. D. Noble, "Separations of Cyclic, Branched, and Linear Hydrocarbon Mixtures Through Silicalite Membranes," *Ind. Eng. Chem. Res.*, **36**, 137 (1997a).

Funke, H. H., K. R. Frender, K. M. Green, J. L. Wilwerding, B. A. Sweitzer, J. L. Falconer, and R. D. Noble, "Influence of Adsorbed Molecules on the Permeation Properties of Silicalite Membranes," *J. Memb. Sci.*, **129**, 77 (1997b).

Furukawa, S., and T. Nitta, "Computer Simulation Studies on Gas Permeation Through Nanoporous Carbon Membranes by Non-Equilibrium Molecular Dynamics," *J. Chem. Eng. Jpn.*, **30**, 116 (1997).

Kapteijn, F., W. J. W. Bakker, G. Zheng, J. Poppe, and J. A. Moulijn, "Permeation and Separation of Light Hydrocarbons Through a Silicalite-1 Membrane, Application of the Generalized Maxwell-Stefan Equations," *Chem. Eng. J.*, **57**, 145 (1995).

Kita, H., "Pervaporation Using Zeolite Membranes," *Proc. Int. Workshop on Zeolitic Membranes and Films*, The Membrane Society of Japan, Tokyo, p. 43 (1998).

Kondo, M., M. Komori, H. Kita, K. Tanaka, and K. Okamoto, "Tubular-Type Pervaporation Module with Zeolite NaA Membrane," *J. Memb. Sci.*, **133**, 133 (1997).

Krishna, R., and J. A. Wesselingh, "The Maxwell-Stefan Approach to Mass Transfer," *Chem. Eng. Sci.*, **52**, 861 (1997).

Krishna, R., and L. P. J. van den Broeke, "The Maxwell-Stefan Description of Mass Transfer Across Zeolite Membranes," *Chem. Eng. J.*, **57**, 155 (1995).

Kusakabe, K., A. Murata, T. Kuroda, and S. Morooka, "Preparation of MFI-type Zeolite Membranes and Their Use in Separating *n*-Butane and *i*-Butane," *J. Chem. Eng. Jpn.*, **30**, 72 (1997a).

Kusakabe, K., T. Kuroda, A. Murata, and S. Morooka, "Formation of a Y-Type Zeolite Membrane on a Porous α-Alumina Tube for Gas Separation," *Ind. Eng. Chem. Res.*, **36**, 649 (1997b).

Kusakabe, K., T. Kuroda, and S. Morooka, "Separation of Carbon Dioxide from Nitrogen Using Ion-Exchanged Faujasite-Type Zeolite Membranes Formed on Porous Support Tubes," *J. Memb. Sci.*, **148**, 13 (1998a).

Kusakabe, K., M. Yamamoto, and S. Morooka, "Gas Permeation and Micropore Structure of Carbon Molecular Sieving Membranes Modified by Oxidation," *J. Memb. Sci.*, **149**, 59 (1998b).

Kusakabe, K., and S. Morooka, "The Use of Zeolite Membranes for the Separation of CO_2," *Proc. Int. Workshop on Zeolitic Membranes and Films*, The Membrane Society of Japan, Tokyo, p. 29 (1998).

Masuda, T., K. Fukuda, Y. Fujikawa, H. Ikeda, and K. Hashimoto, "Measurement and Prediction of the Diffusivities of Y-Type Zeolite," *Chem. Eng. Sci.*, **51**, 1879 (1996).

Morooka, S., S. Yan, K. Kusakabe, and Y. Akiyama, "Formation of Hydrogen Permselective SiO_2 Membrane in Macropores of α-Alumina Support Tube by Thermal Decomposition of TEOS," *J. Memb. Sci.*, **101**, 89 (1995).

Nishiyama, N., K. Ueyama, and M. Matsukata, "Gas Permeation Through Zeolite-Alumina Composite Membranes," *AIChE J.*, **43**, 2724 (1997).

Nomura, M., T. Yamaguchi, and S. Nakao, "Silicalite Membranes Modified by Counterdiffusion CVD Technique," *Ind. Eng. Chem. Res.*, **36**, 4217 (1997).

Nomura, M., T. Yamaguchi, and S. Nakao, "Ethanol/Water Transport Through Silicalite Membranes," *J. Memb. Sci.*, **144**, 161 (1998).

Okazaki, M., H. Tamon, and R. Toei, "Interpretation of Surface Flow Phenomenon of Adsorbed Gases by Hopping Model," *AIChE J.*, **27**, 262 (1981).

Poshusta, J. C., V. A. Tuan, J. L. Falconer, and R. D. Noble, "Synthesis and Permeation Properties of SAPO-34 Tubular Membranes," *Ind. Eng. Chem. Res.*, **37**, 3924 (1998).

Ruthven, D. M., *Principles of Adsorption and Adsorption Process*, Wiley, New York (1984).

Sano, T., S. Ejiri, K. Yamada, Y. Kawakami, and H. Yanagishita, "Separation of Acetic-Water Mixture by Pervaporation Through Silicalite Membrane," *J. Memb. Sci.*, **123**, 225 (1997).

Sea, B. K., K. Kusakabe, and S. Morooka, "Pore Size Control and Gas Permeation Kinetics of Silica Membranes by Pyrolysis of Phenyl-Substituted Ethoxysilanes with Cross-Flow Through a Porous Support Wall," *J. Memb. Sci.*, **130**, 41 (1997).

Talu, O., M. S. Sun, and D. B. Shah, "Diffusivities of *n*-Alkanes in Silicalite by Steady-State Single-Crystal Membrane Technique," *AIChE J.*, **44**, 681 (1998).

Vroon, Z. A. E. P., K. Keizer, M. J. Gilde, H. Verweij, and A. J. Burggraaf, "Transport Properties of Alkanes Through Ceramic Thin Zeolite MFI Membranes," *J. Memb. Sci.*, **113**, 293 (1996).

Vroon, Z. A. E. P., K. Keizer, A. J. Burggraaf, and H. Verweij, "Preparation and Characterization of Thin Zeolite MFI Membranes on Porous Supports," *J. Memb. Sci.*, **144**, 65 (1998).

Manuscript received Aug. 13, 1998, and revision received Apr. 12, 1999.